




# Controlling the Strong Metal-Support Interaction Overlayer Structure in Pt/TiO<sub>2</sub> Catalysts Prevents Particle Evaporation

## Journal Article

### Author(s):

Beck, Arik; Frey, Hannes ; Huang, Xing ; Clark, Adam H.; Goodman, Emmett D.; Cargnello, Matteo; Willinger, Marc ; van Bokhoven, Jeroen A.

### Publication date:

2023-07-03

### Permanent link:

<https://doi.org/10.3929/ethz-b-000616729>

### Rights / license:

[Creative Commons Attribution-NonCommercial 4.0 International](#)

### Originally published in:

Angewandte Chemie. International Edition 62(27), <https://doi.org/10.1002/anie.202301468>

### Funding acknowledgement:

178943 - Catalyst structures in three dimensions (SNF)

181053 - Elektronenmikroskopische Untersuchungen zur Dynamik von Metall- Träger Wechselwirkungen unter katalytisch Relevanten Bedingungen (SNF)

## Heterogeneous Catalysis

# Controlling the Strong Metal-Support Interaction Overlayer Structure in Pt/TiO<sub>2</sub> Catalysts Prevents Particle Evaporation

Arik Beck<sup>+</sup>, Hannes Frey<sup>+</sup>, Xing Huang, Adam H. Clark, Emmett D. Goodman, Matteo Cargnello, Marc Willinger,<sup>\*</sup> and Jeroen A. van Bokhoven<sup>\*</sup>

**Abstract:** Platinum nanoparticles (NPs) supported by titania exhibit a strong metal-support interaction (SMSI)<sup>[1]</sup> that can induce overlayer formation and encapsulation of the NP's with a thin layer of support material. This encapsulation modifies the catalyst's properties, such as increasing its chemoselectivity<sup>[2]</sup> and stabilizing it against sintering.<sup>[3]</sup> Encapsulation is typically induced during high-temperature reductive activation and can be reversed through oxidative treatments.<sup>[1]</sup> However, recent findings indicate that the overlayer can be stable in oxygen.<sup>[4,5]</sup> Using in situ transmission electron microscopy, we investigated how the overlayer changes with varying conditions. We found that exposure to oxygen below 400 °C caused disorder and removal of the overlayer upon subsequent hydrogen treatment. In contrast, elevating the temperature to 900 °C while maintaining the oxygen atmosphere preserved the overlayer, preventing platinum evaporation when exposed to oxygen. Our findings demonstrate how different treatments can influence the stability of nanoparticles with or without titania overlayers, expanding the concept of SMSI and enabling noble metal catalysts to operate in harsh environments without evaporation associated losses during burn-off cycling.

## Introduction

High-temperature oxidative environments are the norm in exhaust gas treatment<sup>[6]</sup> and during burn-off cycles in reactions that are susceptible to heavy coking.<sup>[7,8]</sup> However, many metal catalysts heavily sinter in these conditions. Loss in active surface area of the noble metal component either due to Ostwald ripening or formation of volatile species is

detrimental for catalyst.<sup>[9–11]</sup> Those volatile species form at high temperatures because solid PtO<sub>2</sub> becomes thermodynamic unfavored in oxygen at high temperatures and causes the evaporation of the platinum NPs.<sup>[12–18]</sup> Thus, treatment strategies that allow a catalyst to be exposed to oxygen at high temperatures, but which prevent particle sintering, have the potential to be employed in a large range of catalytic applications. Exploiting the restructuring of catalysts by targeted (pre)treatment is a key concept of virtually all catalytic processes.<sup>[6,7,19]</sup> Either these treatments are applied as preforming step inside a reactor to get the catalyst into a selective and active state<sup>[20,21]</sup> or they can be applied in intervals during the catalytic process to regenerate the deactivated catalyst.<sup>[22]</sup> Supported noble metal NPs, due to scarcity and price of the materials, need to operate at their full potential. Treatments, which alter the catalytic properties of such systems in a desired manner, are consequently subject of intensive research. Supported on reducible oxide carriers, like titania, reductive treatments in hydrogen at elevated temperature (> 400 °C) results in reversible overlayer formation on noble metal NPs,<sup>[23,24]</sup> the so-called strong metal support interaction (SMSI).<sup>[1]</sup> Overlayers strongly influence the catalytic performance and are, for example, used to tune the chemo-selectivity of the catalyst for hydrogenation reactions.<sup>[2,25]</sup> Here, the performance of the catalysts crucially depends on the treatment parameters applied.<sup>[26,27]</sup> Encapsulation can also be used to stabilize the catalyst against deactivation by sintering at high temperature during reaction,<sup>[3,28,29]</sup> or during reoccurring burn-off cycles as to reestablish the catalytic activity.<sup>[30]</sup> As those applications more often than not involve net oxidative environments, the noble metal is especially vulnerable to dissipation and sintering. However, due to the fact that SMSI overlayers are generally believed to be unstable under high temper-

[\*] A. Beck,<sup>+</sup> H. Frey,<sup>+</sup> J. A. van Bokhoven  
Eidgenössische Technische Hochschule Zürich  
Rämistrasse 101, 8092 Zurich (Switzerland)  
E-mail: jeroen.vanbokhoven@chem.ethz.ch

A. Beck,<sup>+</sup> A. H. Clark, J. A. van Bokhoven  
Paul Scherrer Institute  
Forschungsstrasse 111, 5232 Villigen (Switzerland)

X. Huang  
Fuzhou University  
2 Xue Yuan Road, University Town, Fuzhou (P.R. China)

M. Willinger  
Technische Universität München  
Arcisstraße 21, 80333 München (Germany)  
E-mail: marc.willinger@tum.de

E. D. Goodman, M. Cargnello  
Stanford University 450 Serra Mall, Stanford, CA 94305 (USA)

A. Beck<sup>+</sup>  
University of California, Santa Barbara 552 University Rd., Isla Vista,  
CA 93117 (USA)

[<sup>+</sup>] These authors contributed equally to this work.

© 2023 The Authors. Angewandte Chemie International Edition published by Wiley-VCH GmbH. This is an open access article under the terms of the Creative Commons Attribution Non-Commercial License, which permits use, distribution and reproduction in any medium, provided the original work is properly cited and is not used for commercial purposes.

ature in oxidative conditions,<sup>[1]</sup> exploitation of particle encapsulation as a strategic protective mechanism against particle dissipation is an application much less explored. Nonetheless and in contrast to the general assumption of instability in oxygen,<sup>[1,31]</sup> recent studies show that the overlayer is stable<sup>[4]</sup> or may even form in oxygen above 400 °C.<sup>[32,33]</sup> The overlayer can be destabilized at 600 °C in a redox-active atmosphere that contains both, oxygen and hydrogen. As a consequence, particles become dynamic and mobile. Subsequent retraction of hydrogen leads to re-encapsulation.<sup>[34]</sup> In situ transmission electron microscopy (TEM) has proven potential to monitor formation, retraction and reformation of overlayers and their structure.<sup>[31,35,36]</sup> Here, we followed surface transformation and encapsulation in oxygen between room temperature and 800 °C. Direct observation was complemented with in situ X-ray absorption spectroscopy (XAS). It was found that the surface oxidation state of platinum is critical for the stability of titania overlayers. At high temperatures, the overlayer is stable in 200 mbar of oxygen and prevents the platinum NPs from dissipation. In contrast, cooling the encapsulated catalyst to 400 °C in oxygen leads to the formation of a platinum surface oxide and the retraction of the titania overlayer. Reheating the catalyst to temperatures of 600 °C and above renders platinum oxide thermodynamically unfavorable with respect to metallic platinum and during its reduction, the particle becomes re-encapsulated by titania. Thus, protective encapsulating titania layers are stable in oxygen only above a temperature where metallic platinum is the thermodynamically preferred termination with respect to its oxide. This current work on the one hand harmonizes discrepancies between recent observations of oxygen induced particle overlayers and the original SMSI protocol<sup>[1]</sup> and, on the other, identifies a way to apply high-temperature oxidative treatments without particle evaporation and sintering.

## Results and Discussion

Platinum NP (15 nm) were synthesized by colloidal synthesis and deposited on titania.<sup>[37]</sup> The fresh catalyst presented platinum nanoparticles with a clean surface (Supporting Figure S1). The sample was heated up in an oxygen mixture (20 % O<sub>2</sub>/He), in situ, during transmission electron microscopy using a MEMS-based micro reactor (Figure 1). At 400 °C, an ill-structured surface layer developed. This layer is visible in both the high-angle annular dark field (HAADF) and the annular bright field (ABF) of the scanning transmission electron microscopy (STEM) images. The comparison of HAADF and ABF is helpful to understand the composition of the overlayers. HAADF images are much more sensitive to high masses in the imaged materials (Z-contrast), while ABF is advantageous for light material contrast. HAADF imaging revealed that the overlayer formed at 400 °C in oxygen shows bright features and therefore, presumably contains platinum (Figure 1a). When the catalyst is heated further to 600 °C, the surface structure transforms again (Figure 1c,d). In this state, a much more defined and ordered surface structure is

observed in the ABF image that strongly resembles a previously reported structure.<sup>[4]</sup> In this state, the corresponding HAADF image (Figure 1c) shows weak contrast in the overlayer. Lattice space analysis of the NP (Figure 1i, Supporting Figure S2) shows that the outer two layers have a similar lattice spacing of 0.3 nm, a reasonably good match for both, PtO<sub>2</sub> and TiO<sub>2</sub>. In this process, it was observed that the formation of the well-structured overlayer on the platinum NPs coincided with a restructuring of the whole platinum NPs: They became more faceted in comparison to the previously round shape (Supporting Figure S3). Multi-slice simulations on TiO<sub>2</sub> as well as  $\beta$  PtO<sub>2</sub> overlayers were performed in order to assess the large contrast difference in HAADF (Supporting Figure S4). The results validate weak contrast in the applied HAADF imaging conditions in case of the TiO<sub>2</sub> overlayer while the  $\beta$  PtO<sub>2</sub> overlayer is clearly visible. Furthermore, presence of titania was confirmed by EELS line-scans (recorded along the overlayer area, Supporting Figure S5). These observations suggest that the particle termination transformed from a disordered state to being covered by a titania overlayer. In a complementary in situ XAS experiment, the catalyst was heated in the same gas composition (20 % O<sub>2</sub>/He) stepwise from room temperature to 750 °C. During the experiment, small changes in the structure of the Pt L<sub>3</sub>-edge were observed (Figure 1g, Supporting Figure S6). Initially, the white line intensity increased up to a temperature of 300 °C. Then, its intensity dropped until the temperature reached 500 °C. Beyond this temperature, there are no changes in the Pt L<sub>3</sub>-edge. Linear combination fitting (LCF) was performed with a metallic platinum and a platinum(IV) oxide reference (Figure 1h). The results show that platinum partially oxidizes when heated up, resulting in around 1.2 % Pt<sup>4+</sup> at 300 °C. A NP with a diameter of 15 nm exposes around 5–8 % of its atoms.<sup>[38]</sup> Assuming that the oxidized platinum species are located at the particle surface, this value of 1.2 % Pt<sup>4+</sup> corresponds, thus, to around 15–24 % of a mono surface layer of platinum(IV) oxide. Thus, the disordered overlayer observed in oxygen at 300 °C is likely a surface platinum oxide.<sup>[15,18]</sup> Beyond 300 °C, platinum gradually reduces to a fully metallic state with no further changes in the Pt L<sub>3</sub>-edge above 500 °C, in line with literature data.<sup>[13–18]</sup> The examination of the extended X-ray absorption fine structure (EXAFS) region yielded no significant changes (see Supporting Figure S7&S8). The XAS results thus support the STEM findings and show that platinum reduction and titania overlayer formation coincide.

These experiments evidence that overlayer formation may occur without the presence of hydrogen, provided the conditions are such that the metal is in a reduced state.<sup>[32]</sup> This is also in line with the observation of a stable overlayer in oxygen for platinum-titania catalysts when switching from a hydrogen atmosphere to an oxygen environment at 600 °C<sup>[4]</sup> or when retracting hydrogen from a mix of hydrogen and oxygen.<sup>[34]</sup> However, the original protocol<sup>[1]</sup> reported the restoration of noble metal chemisorption capacity after high temperature oxidative and low temperature reductive treatment. Consequently, and to elucidate this apparent discrepancy, the catalyst was cooled down to

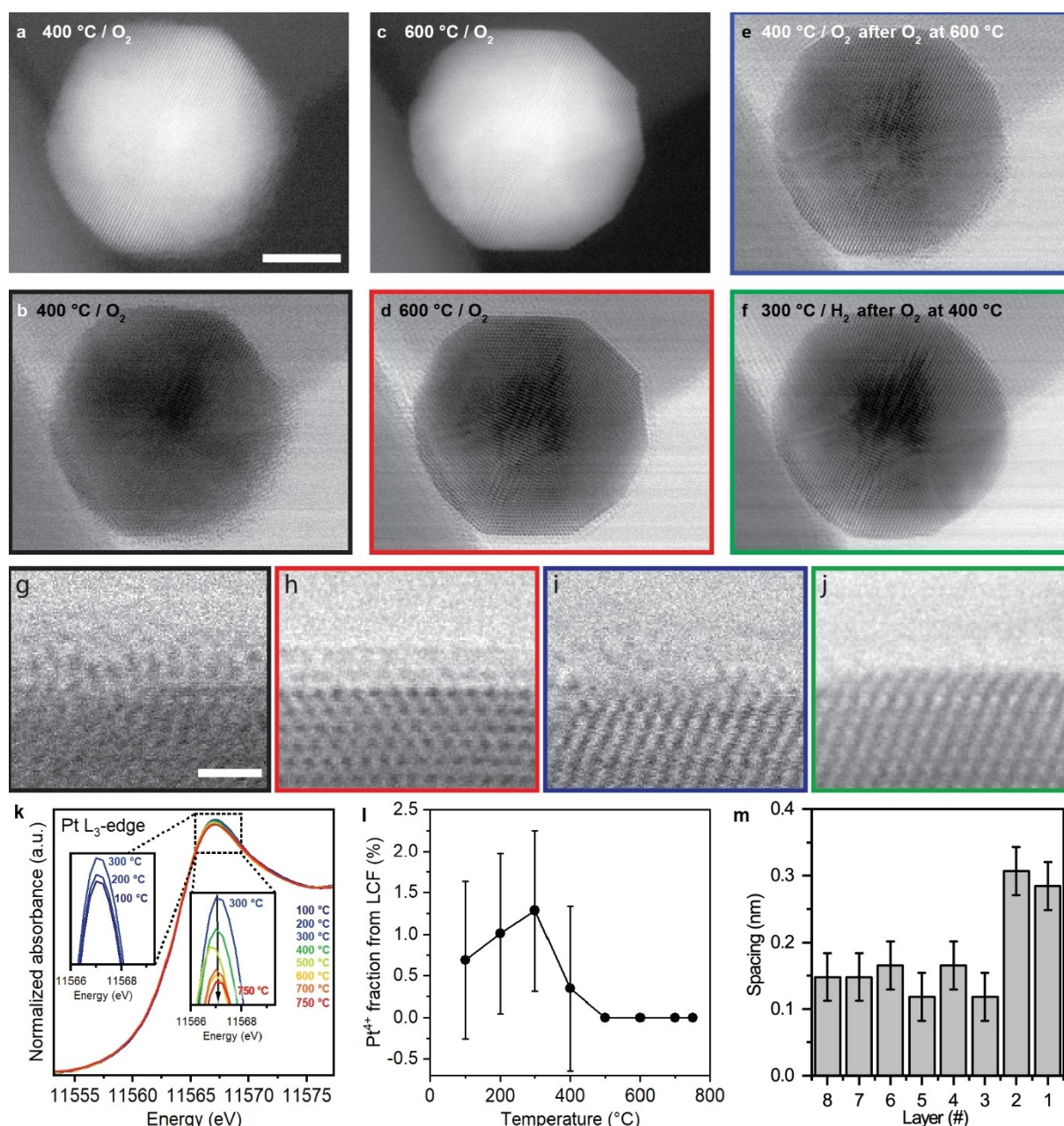


**Figure 1.** Overlayer formation in 200 mbar of oxygen: Platinum nanoparticle in oxygen at 400 °C: a) high-angle annular dark field (HAADF) and b) annular bright-field (ABF). The same platinum nanoparticle after heating in oxygen to 600 °C: c) HAADF and d) ABF. e) ABF of the platinum nanoparticle in oxygen at 400 °C after treatment in oxygen at 600 °C. f) ABF of the particle after 30 min exposure to hydrogen at 300 °C. g)–j) magnified detail of the particle termination. Frame color corresponds to (b, d, e, f). k) In situ Pt L<sub>3</sub>-edge XANES of the catalyst stepwise heated in oxygen to 750 °C. l) Linear combination fitting results for the Pt<sup>4+</sup> component as a function of temperature. m) Lattice space analysis of the outward top 8 lattice planes of the platinum particle in oxygen at 600 °C in panel (d) and Supporting Figure S2. The oxygen gas composition was in all experiments 20% O<sub>2</sub> balanced in He and for hydrogen 100% H<sub>2</sub>. Reactor pressure is 1 bar, scale bar corresponds to 5 nm in (a) with (a–f) being at the same magnification and 1 nm in (g) with (g–j) at the same magnification.

400 °C in 20% O<sub>2</sub>/He (Figure 1e). During cooldown, the surface of the platinum particles again became disordered. This structure appears very similar to the initial surface structure seen at 400 °C during heating the catalyst in 200 mbar O<sub>2</sub> (Figure 1a, b). This resemblance can be interpreted as a surface oxidation of platinum (Energy dispersive X-ray spectroscopy (EDX) mapping of the particle is

provided in Supporting Figure S9). Subsequently, the reactor was flushed with helium and cooled to 300 °C. At this temperature, hydrogen was introduced into the reactor. The platinum surface transformed again into an ordered crystal structure (Figure 1f).

The observed changes in response to the sequence of applied conditions allows us to understand, why the



oxidative treatment described in the original work by Tauster et al.<sup>[1]</sup> led to an efficient removal of the overlayer. Exposing an encapsulated catalyst to oxygen at temperatures  $\approx 400^\circ\text{C}$  will oxidize the platinum surface. As the interaction strength of a fully oxidized titania layer and oxidized platinum is presumably very weak<sup>[4,39,40]</sup> and surface oxidation is accompanied by particle surface reconstruction (Figure 1a,c), the titania overlayer is meanwhile destabilized and removed. In the last step, the hydrogen reduction at

milder temperatures ( $300^\circ\text{C}$ ) restores the metallic platinum surface.

In a subsequent experiment, a freshly prepared sample was directly heated in 20 %  $\text{O}_2/\text{He}$  to  $600^\circ\text{C}$ . Then the catalyst was heated further to  $800^\circ\text{C}$  and was kept at this temperature for 800 s (Figure 2a, Movie S1). The diameter of all NPs in the frame were tracked in this time period using a U-net type<sup>[41]</sup> convolutional network. No size change

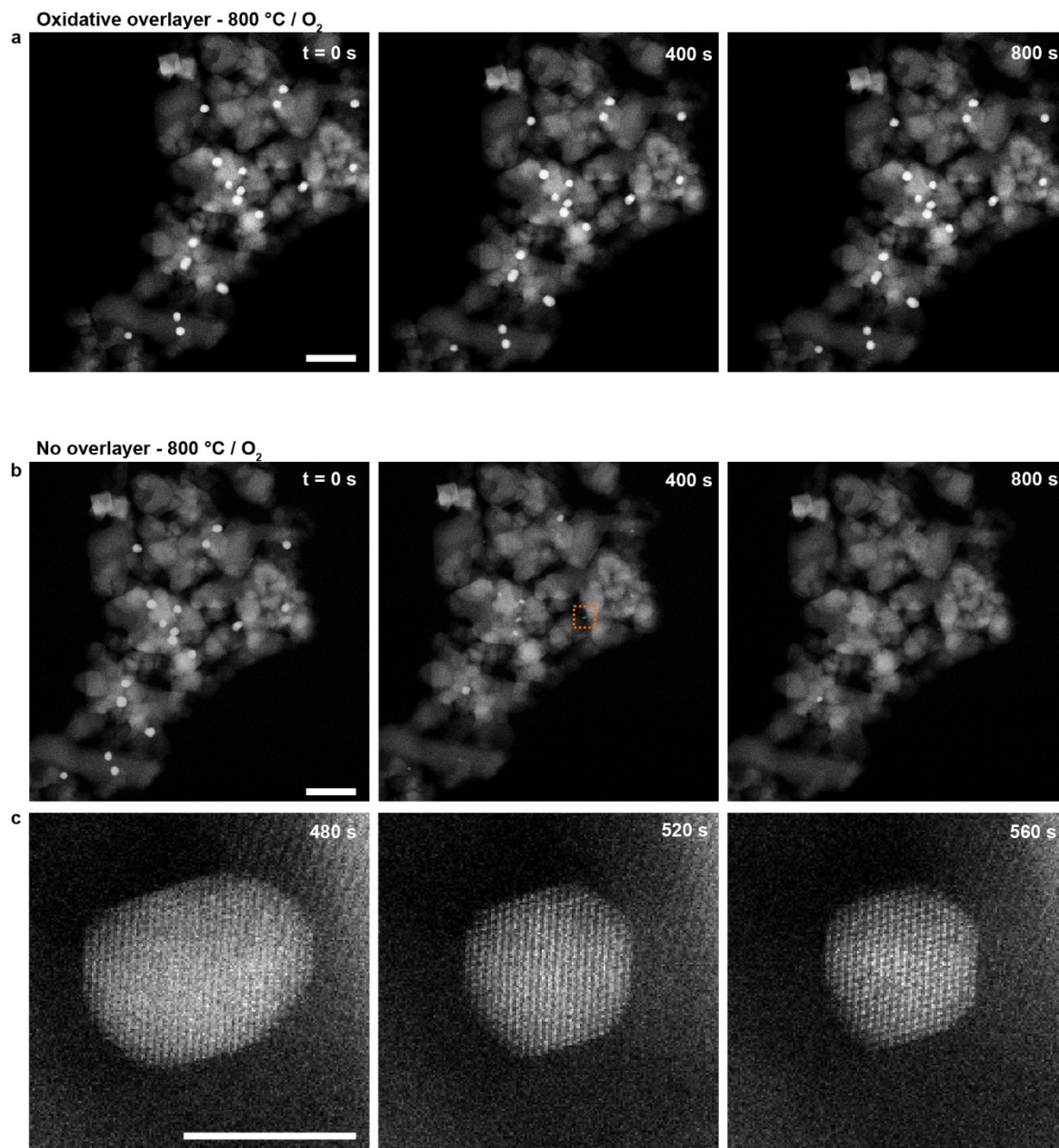


**Figure 2.** Overlayer protects against evaporation: A platinum-titania catalyst was heated in 20%  $\text{O}_2/\text{balance He}$  to  $600^\circ\text{C}$  and subsequently to  $800^\circ\text{C}$ . a) The evolution of the platinum nanoparticles at  $800^\circ\text{C}$  was followed for 800 s (HAADF micrographs). b) The overlayer was removed by cooling 'to  $600^\circ\text{C}$  in 20%  $\text{O}_2/\text{balance He}$  and a subsequent switch to 19.6%  $\text{O}_2/0.4\% \text{H}_2/\text{He}$  for 10 min. After overlayer removal, the gas atmosphere was switched back to 20%  $\text{O}_2/\text{balance He}$  and the catalyst was heated back to  $800^\circ\text{C}$ . After reheating, the same catalyst grain was studied for 1200 s (b). During observation, all nanoparticles but one shrunk and disappeared. c) For a time period ( $t=475\text{--}580\text{ s}$ ), one particle (red box in b) was followed in high resolution. Reactor pressure at all times was 1 bar, scale bar in (a) and (b) is 100 nm and in (c) 5 nm.

Supporting Information Figure S8, high resolution STEM imaging at 800 °C in Supporting Information Figure S11). Remarkably, no change in particle size could be detected even when the catalyst was exposed to harsher conditions, i.e., at 900 °C to 1 bar of oxygen (Supporting Figure S10, Movie S2). Recently, it was observed that, at 600 °C, a mixture of oxygen with small amounts of hydrogen is able to strip the titania overlayer off the platinum particle.<sup>[34]</sup> Therefore, the catalyst was cooled to 600 °C and a small amount of hydrogen was added to the gas mixture (19.6 % O<sub>2</sub>/0.4 % H<sub>2</sub>/He) for 10 min. After de-encapsulation, hydrogen was retracted and the catalyst quickly heated to 800 °C (heating ramp 100 °C min<sup>-1</sup>) in oxygen, reaching the exact same conditions as before (Figure 2a). Figure 2b displays snapshots from a time series taken at the same region of interest as in Figure 2a. In contrast to the previous experiment with the encapsulated particles, the particles without protective overlayer decrease in size (Movie S3). The difference in behavior is a nice example for the often stated memory effect of previous treatments. High resolution imaging of a particle during dissipation is shown in Figure 2c. Within 800 s, all NP except one had disappeared (Figure 2b, Supporting Figure S10). Dissipation of the platinum NPs is assumed to occur via PtO<sub>x</sub> formation, a species that is volatile at high temperatures.<sup>[10,42]</sup> Within the in situ TEM microreactor cell, volatile PtO<sub>x</sub> may easily anchor on other surface like the reactor wall instead of on catalyst grains. Within our experiments, we could not determine the new location of the platinum species.

In order to examine potential artifacts due to the electron beam. A second region of the sample had been measured with minimal beam exposure in low magnification at the beginning of the experiment, at 900 °C in 200 mbar O<sub>2</sub> when no Pt evaporation had been observed, and at the end of the Pt evaporation period in 800 °C in 200 mbar O<sub>2</sub>. The results are depicted in Supporting Figure S12. These results show similar results and suggest that the overall phenomena were not substantially altered by the electron beam. Particle evaporation and overlayer reformation likely comprise two competing mechanisms when the sample is again exposed to pure oxygen after overlayer removal. The formation of volatile species is strongly dependent on applied temperature and oxygen pressure.<sup>[1]</sup> It is thus reasonable to assume that altering those process variables could lead to particles re-encapsulating after initial shrinking in size via evaporation processes. Indeed, during the experiment, one particle remained visible throughout. ABF imaging and repeated experiments (Supporting Information Figure S13), indicate that re-encapsulation is hindering further evaporation in those cases. However, additional investigations are needed to investigate the kinetic competition of particle evaporation and overlayer (re)formation.

These experiments show that an oxidatively-formed titania overlayer is an effective way to prevent platinum dissipation at high temperatures. Figure 3 summarizes the structural development of the platinum NPs and overlayer as function of condition and sample history<sup>[4,34]</sup> (labeled as states I–VIII). In the as-prepared state (I) platinum NPs on titania do not have any overlayer of titania. The platinum-

titania catalyst can be either stable (IV) or labile (V) at 800 °C in 20 % O<sub>2</sub>/He. The stability is determined by the sequence of conditions the catalyst was exposed to, prior to high-temperature exposure. Similarly, the seeming discrepancy between the reported presence of an overlayer at 600 °C in oxygen (III) and the observed removal upon an oxygen treatment at 400 °C (II) emerges from the details in the experimental protocols. Overlayer structures at 400 °C (II) and 600 °C (III) in oxygen are substantially different from each other.

An ordered overlayer is only stable in oxygen above the decomposition temperature of platinum surface oxide ( $\approx 400$  °C) and consequently can only be detected by in situ characterization methods. Classical methods to characterize SMSI overlayers are CO-infrared experiments and chemisorption studies.<sup>[25]</sup> Such methods require low temperature and the exposure of the catalyst to different gases. Therefore, any original overlayer structure is not preserved and, consequently, cannot be studied.

The observation of an overlayer formation in oxidizing conditions can be rationalized by considering the prerequisites for overlayer formation: i) Thermodynamics have to drive the encapsulation process, and ii) TiO<sub>x</sub> ( $x=0-2$ ) has to be sufficiently mobile in order to migrate onto the NP surface. Exposure to high temperatures induces ion mobility, increases the amount of oxygen vacancies within titania<sup>[44]</sup> and consequently, the concentration of Ti<sup>3+</sup> cations. This is particularly valid at the particle support interface where oxygen vacancy formation can relieve strain introduced by the heterogeneous interface itself.<sup>[45–48]</sup> These Ti<sup>3+</sup> cations also exist in oxygen atmospheres and form strong bonds with reduced platinum surfaces.<sup>[4,40]</sup> This strong bond formation in concert with the thermodynamic desired minimization of surface energy<sup>[49,50]</sup> induces the overlayer in oxygen. Recently, Petzoldt et al. showed that TiO<sub>x</sub> overlayer formation dynamics depend sensitively on the oxygen pressure as it dictates the oxidation state of platinum. Once a titania overlayer is formed, it effectively protects the particle against evaporating via the formation of volatile PtO<sub>2</sub> monomers.<sup>[10]</sup> Removal of the overlayer at temperatures above the decomposition temperature of PtO<sub>x</sub> realized by the exposure to a reductant or a reactive hydrogen-oxygen mixture<sup>[34]</sup> results in removal of the protective encapsulating layer and makes platinum particles vulnerable for evaporation (VI). When the temperature is reduced in the overlaid state, the formation of a solid PtO<sub>x</sub> surface layer becomes favorable (II). Oxidation of platinum leads to the destruction of the well ordered TiO<sub>x</sub> overlayer and leaves the particle in a yet undefined, partially oxidized surface state, that then can be transformed to clean platinum by hydrogen (VII). In order to evaluate consequences of this encapsulation behaviour for a catalytic reaction, a series of CO oxidation light-off experiments was performed. In these experiments, several sequential treatments resembling those of the in situ TEM experiment were performed and in between the catalytic activity for CO oxidation was evaluated. The results are shown and discussed in detail in Supporting Figure S14. In summary, the catalyst lost a substantial degree of activity after treatments at 600 °C and

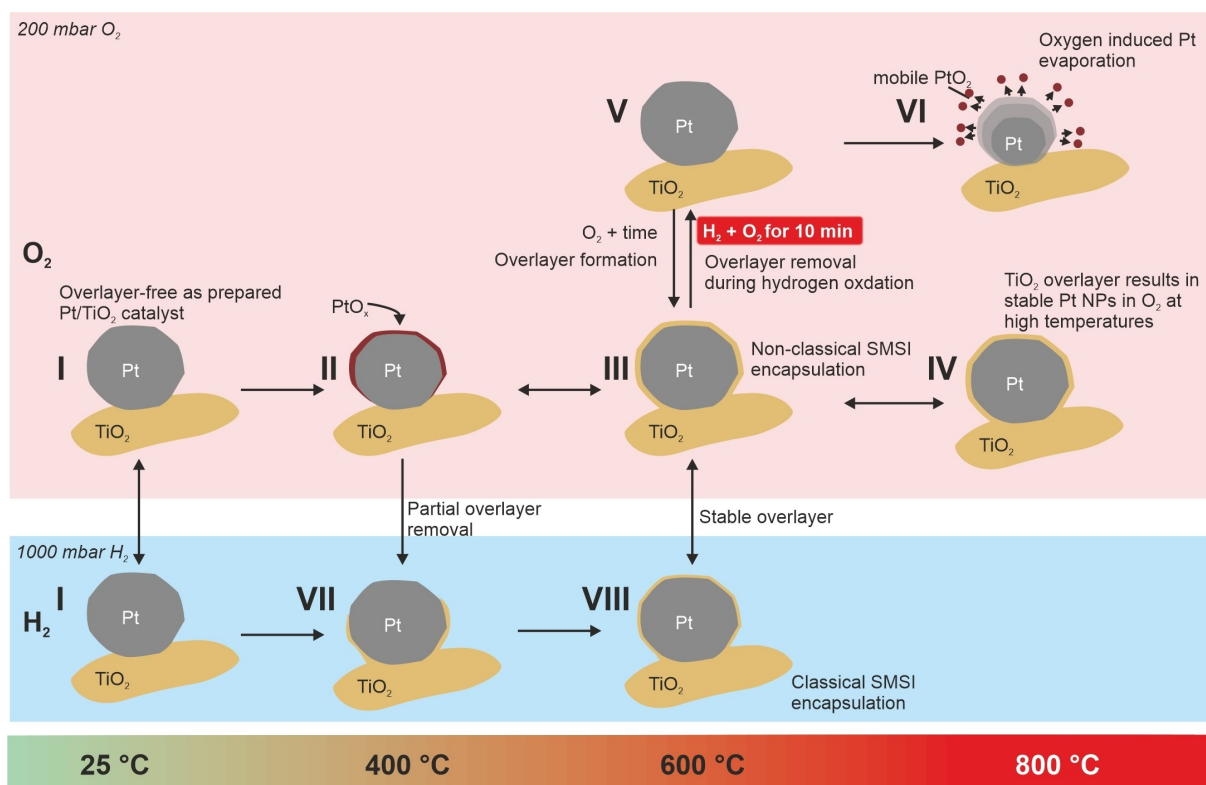


**Figure 3.** Evolution of the platinum-titania catalyst as function of conditions: By a sequence of in situ experiment, the structure of platinum particle surfaces was followed. Based on the observations a behavior pattern of the surface structure can be determined. Certain changes in atmospheric conditions (temperature and gas composition) result in reversible structural transformations (double arrow). Other atmospheric changes result in irreversible transformations of the catalysts surface (single arrow).

in 200 mbar  $O_2$ . However, a treatment at 400 °C and in 200 mbar  $O_2$ , followed by a 1 bar  $H_2$  reduction at 300 °C fully restored the activity of the catalyst. The data supports the proposition that the overlayer is formed under oxygen and is detrimental for the CO oxidation activity. Nevertheless, by following the treatment proposed in Figure 3, the activity can be fully restored, indicating that the size and number of platinum NPs is not changing by these treatments.

Yet, the sample studied within this work is composed of large NPs. SMSI related phenomena have been shown to be sensitive to the metal NP size.<sup>[51]</sup> Therefore, how these findings directly apply to smaller platinum NPs must be further evaluated.

## Conclusion

The present work investigated the impact of (pre)treatment protocols of a Pt/TiO<sub>2</sub> catalyst on the formation and structure of overlayers and the occurrence of platinum evaporation during exposure to high-temperature oxidative conditions. The current work expands the conceptual understanding of the SMSI state and shows why the overlayer that is formed in oxygen at high temperatures cannot be observed using ex situ characterization, since it is only stable in oxygen above 400 °C. An overlayer protects platinum against dissipation at high temperatures (up to 900 °C) and

oxygen pressures up to 1 bar. The presence of a protective overlayer depends on the treatment history of the sample, and requires that the catalyst is kept in oxygen from below 400 °C to 600 °C. Our results highlight how critically each step during catalysis treatment impacts the desired material properties, specifically in forming a protective encapsulation layer that effectively protects platinum particles from dissipation or sintering during exposure to high temperature oxidative environments.

## Acknowledgements

We thank Mark A. Newton and Ilia Sadykov for the support during beamtime and Ali Baghi Zadeh and Xing Wang for the support with multi-slice STEM simulations. Further we acknowledge the Swiss Light Source (SLS), especially the SuperXAS beamline, for the provision of XAS beamtime (proposal no. 20201787). We thank the Scientific Center for Optical and Electron Microscopy (ScopeM) at ETH Zurich for the electron microscopy access. A.B. and J.A.v.B. acknowledge the SNSF project 200021\_178943 and H.F. and M.G.W. acknowledge the SNSF project 200021\_181053 for the financial support. Open Access funding provided by Eidgenössische Technische Hochschule Zürich.



## Conflict of Interest

The authors declare no conflict of interest.

## Data Availability Statement

The data that support the findings of this study are available in the Supporting Information of this article.

**Keywords:** Electron Microscopy • Heterogeneous Catalysis • Metal-Support Interaction • Platinum

- [1] S. J. Tauster, S. C. Fung, R. L. Garten, *J. Am. Chem. Soc.* **1978**, *100*, 170–175.
- [2] A. Corma, P. Serna, P. Concepción, J. J. Calvino, *J. Am. Chem. Soc.* **2008**, *130*, 8748–8753.
- [3] E. D. Goodman, J. A. Schwalbe, M. Cargnello, *ACS Catal.* **2017**, *7*, 7156–7173.
- [4] A. Beck, X. Huang, L. Artiglia, M. Zabilskiy, X. Wang, P. Rzepka, D. Palagin, M.-G. Willinger, J. A. van Bokhoven, *Nat. Commun.* **2020**, *11*, 3220.
- [5] M. Tang, S. Li, S. Chen, Y. Ou, M. Hiroaki, W. Yuan, B. Zhu, H. Yang, Y. Gao, Z. Zhang, Y. Wang, *Angew. Chem. Int. Ed.* **2021**, *60*, 22339–22344.
- [6] E. S. J. Lox, *Handbook of Heterogeneous Catalysis*, Wiley-VCH, Weinheim, **2008**, pp. 2274–2345.
- [7] J. A. Moulijn, A. E. van Diepen, F. Kapteijn, *Handbook of Heterogeneous Catalysis*, Wiley-VCH, Weinheim, **2008**.
- [8] O. Muraza, A. Galadima, *Int. J. Energy Res.* **2015**, *39*, 1196–1216.
- [9] S. B. Simonsen, I. Chorkendorff, S. Dahl, M. Skoglundh, J. Sehested, S. Helveg, *J. Am. Chem. Soc.* **2010**, *132*, 7968–7975.
- [10] P. N. Plessow, F. Abild-Pedersen, *ACS Catal.* **2016**, *6*, 7098–7108.
- [11] E. D. Goodman, A. C. Johnston-Peck, E. M. Dietze, C. J. Wrasman, A. S. Hoffman, F. Abild-Pedersen, S. R. Bare, P. N. Plessow, M. Cargnello, *Nat. Catal.* **2019**, *2*, 748–755.
- [12] J. Oh, A. Beck, E. D. Goodman, L. T. Roling, A. Boucly, L. Artiglia, F. Abild-Pedersen, J. A. van Bokhoven, M. Cargnello, *ACS Catal.* **2023**, *13*, 1812–1822.
- [13] L. Brewer, *Chem. Rev.* **1953**, *52*, 1–75.
- [14] C. A. Krier, R. I. Jaffee, *J. Less-Common Met.* **1963**, *5*, 411–431.
- [15] J. C. Chaston, *Platinum Met. Rev.* **1964**, *8*, 50–54.
- [16] R. J. Berry, *Can. J. Chem.* **1977**, *55*, 1792–1793.
- [17] H. Jehn, *J. Less-Common Met.* **1984**, *100*, 321–339.
- [18] L. K. Ono, B. Yuan, H. Heinrich, B. R. Cuenya, *J. Phys. Chem. C* **2010**, *114*, 22119–22133.
- [19] F. Schüth, M. Hesse, K. K. Unger, *Handbook of Heterogeneous Catalysis*, Wiley-VCH, Weinheim, **2008**, pp. 100–119.
- [20] M. Behrens, R. Schlögl, *Z. Anorg. Allg. Chem.* **2013**, *639*, 2683–2695.
- [21] A. Beck, M. A. Newton, M. Zabilskiy, P. Rzepka, M. G. Willinger, J. A. van Bokhoven, *Angew. Chem. Int. Ed.* **2022**, *61*, e202200301.
- [22] A. M. Gänzler, M. Casapu, P. Vernoux, S. Lorient, F. J. C. S. Aires, T. Epicier, B. Betz, R. Hoyer, J.-D. Grunwaldt, *Angew. Chem. Int. Ed.* **2017**, *56*, 13078–13082.
- [23] E. J. Braunschweig, A. D. Logan, A. K. Datye, D. J. Smith, *J. Catal.* **1989**, *118*, 227–237.
- [24] S. Bernal, F. J. Botana, J. J. Calvino, C. López, J. A. Pérez-Omil, J. M. Rodríguez-Izquierdo, *J. Chem. Soc. Faraday Trans.* **1996**, *92*, 2799–2809.
- [25] M. Macino, A. J. Barnes, S. M. Althahban, R. Qu, E. K. Gibson, D. J. Morgan, S. J. Freakley, N. Dimitratos, C. J. Kiely, X. Gao, A. M. Beale, D. Bethell, Q. He, M. Sankar, G. J. Hutchings, *Nat. Catal.* **2019**, *2*, 873–881.
- [26] Y. Zhang, X. X. Yang, X. X. Yang, H. Duan, H. Qi, Y. Su, B. Liang, H. Tao, B. Liu, D. Chen, X. Su, Y. Huang, T. Zhang, *Nat. Commun.* **2020**, *11*, 3185.
- [27] J. C. Matsubu, S. Zhang, L. DeRita, N. S. Marinkovic, J. G. Chen, G. W. Graham, X. Pan, P. Christopher, *Nat. Chem.* **2017**, *9*, 120–127.
- [28] S. Liu, W. Xu, Y. Niu, B. Zhang, L. Zheng, W. Liu, L. Li, J. Wang, *Nat. Commun.* **2019**, *10*, 5790.
- [29] H. Wang, L. Wang, D. Lin, X. Feng, Y. Niu, B. Zhang, F.-S. Xiao, *Nat. Catal.* **2021**, *4*, 418–424.
- [30] D. L. Trimm, *Appl. Catal. A* **2001**, *212*, 153–160.
- [31] S. Zhang, P. N. Plessow, J. J. Willis, S. Dai, M. Xu, G. W. Graham, M. Cargnello, F. Abild-Pedersen, X. Pan, *Nano Lett.* **2016**, *16*, 4528–4534.
- [32] P. Petzoldt, M. Eder, S. Mackewicz, M. Blum, T. Kratky, S. Günther, M. Tschurl, U. Heiz, B. A. J. Lechner, *J. Phys. Chem. C* **2022**, *126*, 16127–16139.
- [33] H. Tang, Y. Su, Y. Guo, L. Zhang, T. Li, K. Zang, F. Liu, L. Li, J. Luo, B. Qiao, J. Wang, *Chem. Sci.* **2018**, *9*, 6679–6684.
- [34] H. Frey, A. Beck, X. Huang, J. A. van Bokhoven, M. G. Willinger, *Science* **2022**, *376*, 982–987.
- [35] M. Tang, W. Yuan, Y. Ou, G. Li, R. You, S. Li, H. Yang, Z. Zhang, Y. Wang, *ACS Catal.* **2020**, *10*, 14419–14450.
- [36] M. Boniface, M. Plodinec, R. Schlögl, T. Lunkenbein, *Top. Catal.* **2020**, *63*, 1623–1643.
- [37] M. Cargnello, *Chem. Mater.* **2019**, *31*, 576–596.
- [38] D. Oh, Y.-J. Lee, K.-Y. Lee, J.-S. Park, *Catalysts* **2020**, *10*, 1283.
- [39] J. A. Horsley, *J. Am. Chem. Soc.* **1979**, *101*, 2870–2874.
- [40] X. Wang, A. Beck, J. A. van Bokhoven, D. Palagin, *J. Mater. Chem. A* **2021**, *9*, 4044–4054.
- [41] O. Ronneberger, P. Fischer, T. Brox, *18<sup>th</sup> International Conference on Medical Image Computing and Computer Assisted Intervention*, **2015**, pp. 234–241.
- [42] J. Jones, H. Xiong, A. T. DeLaRiva, E. J. Peterson, H. Pham, S. R. Challa, G. Qi, S. Oh, M. H. Wiebenga, X. I. P. Hernández, Y. Wang, A. K. Datye, *Science* **2016**, *353*, 150–154.
- [43] H. Jehn, *J. Less-Common Met.* **1981**, *78*, 33–41.
- [44] M. A. Henderson, *Surf. Sci.* **1999**, *419*, 174–187.
- [45] R. A. Bennett, P. Stone, M. Bowker, *Catal. Lett.* **1999**, *59*, 99–105.
- [46] P. Müller, R. Kern, *Surf. Sci.* **2000**, *457*, 229–253.
- [47] C. Castellarin-Cudia, S. Surnev, G. Schneider, R. Podlucky, M. G. Ramsey, F. P. Netzer, *Surf. Sci.* **2004**, *554*, L120–L126.
- [48] A. Ruiz Puigdollers, P. Schlexer, S. Tosoni, G. Pacchioni, A. R. Puigdollers, P. Schlexer, S. Tosoni, G. Pacchioni, *ACS Catal.* **2017**, *7*, 6493–6513.
- [49] L. Vitos, A. V. Ruban, H. L. Skriver, J. Kollár, *Surf. Sci.* **1998**, *411*, 186–202.
- [50] A. S. M. Jonayat, S. Chen, A. C. T. Van Duin, M. Janik, *Langmuir* **2018**, *34*, 11685–11694.
- [51] Y. Zhang, J. Liu, K. Qian, A. Jia, D. Li, L. Shi, J. Hu, J. Zhu, W. Huang, *Angew. Chem. Int. Ed.* **2021**, *60*, 12074–12081.

Manuscript received: January 30, 2023

Accepted manuscript online: May 4, 2023

Version of record online: May 19, 2023